An Equation for Bubble-Induced Voltage Drop on Slotted and Non-Slotted Anodes

Vanderlei Gusberti[1] and Dagoberto Schubert Severo[2]
1. PhD Engineer
2. Director
CAETE Engenharia, Porto Alegre, Brazil
Corresponding author: vanderlei@caetebr.com
https://doi.org/10.71659/icsoba2025-al055

Abstract

The standard industrial aluminium electrolysis process relies on consumable carbon anodes, where the carbon is oxidized, generating mostly CO_2 at the anode bottom surface, forming bubbles inside the electrolyte. The presence of the bubbles is undesired because it increases the Anode-to-Cathode Distance (ACD) voltage drop, thus increasing the cell specific energy consumption. These bubbles are removed from anode bottom and discharged at the bath top surface, at the sides and in between anode channels.

Previous Computational Fluid Dynamic (CFD) simulations [1] have demonstrated that the anode geometrical features such as: anode size and inclination, number and size of slots, and edge-rounding radius strongly impact the bubble flow and the resulting ACD voltage drop. Slotted anodes have become the standard design in the industry in this century, because the gas removal from ACD space is more efficient, reducing the voltage drop caused by bubbles. However, it is very difficult to quantitatively determine the impact of slots on ACD voltage drop without numerical modelling; which usually requires prototyping and extensive data measurements and processing. It would therefore be highly beneficial if such estimation could be made using published analytical equations.

This work proposes the development of analytical equations estimating bubble-induced voltage drop for slotted and non-slotted anodes, capable of considering a range of geometrical anode features such as anode length, width, channel height, nominal current density, slot width, slot height and others. The analytical equations are derived from detailed 3D multiphase CFD results where transient bubble structures can be followed along their paths, including growth, coalescence, and detachment from the anode surface. This provides a quick tool for design evaluation by process engineers, without the need for intensive computational power. The present work results are compared with classical literature formulae compilations [2], developed for non-slotted anodes which were standard at that time.

Keywords: Bubble voltage equation, Slotted anode, Anode shape, Bubble-induced voltage drop, Bubble-induced flow.

1. Introduction

Most of the modern aluminium electrolysis cells utilize carbon blocks as consumable anodes, taking advantage of the carbon oxidation contributing to the fulfilment of energy requirements for alumina reduction, and decreasing the electrical energy input compared to inert anodes. These carbon blocks are placed inside the cell, arranged in a horizontal array over the cathode panel and the bath. The electrical current flows through the anode, molten bath ACD, and molten metal into the cathode panel. In such a configuration, the gas (mostly CO_2 and CO) generated beneath the anode bottom surface forms bubbles which travel attached to that surface. Because the gas is an electrical insulator, it disturbs the path of current lines and reduces the local effective area for

electrical conduction from anode to bath, covering part of anode surface area. The continuous removal of the gas under the anode surface is a difficult and complex process, and it is important for the decreasing of the bath bulk voltage drop. The bubbles must escape from the ACD space where they are formed and travel towards the anode sides and bath channels where they can be discharged to the cell hood space and then collected by the cell exhaust system. The driving force for such movement is the buoyancy, which is generated from the significant difference in density between gas and bath. In this perspective, the study and understanding of the bubble flow inside the bath is important for improving anode design and configuration to minimize bubble-induced voltage drop which is closely related to the bubble removal efficiency.

The bubbles present a life cycle inside the bath composed of nucleation, growth, coalescence and detachment processes leading to a complex multiphase flow in the ACD space, side and center channels. A numerical model capable of describing this process was presented in an earlier work [1] and the model was also used to calculate the voltage drop induced by bubbles inside the bath. One of the conclusions of the previous modelling work was that the shape of the anode bottom surface significantly affects the voltage drop outcome, and the modelling must consider realistic consumed shapes to obtain meaningful results. The shape can be obtained from measurements of real consumed carbon blocks (as presented in [1]) or from numerical modelling results. A consumed anode usually presents a rounding shape formed during the anode life in the cell due to the concentration of electrical current and the resulting higher wearing rate at sharp edges, therefore equalizing the current density across the entire anode bottom surface. The stabilized anode bottom shape and edge curvature are dependent on anode current density distribution; which in turn is a function of the ohmic, bubbles, chemical decomposition and polarisation voltages.

The use of consumable slotted anodes has become a standard industrial practice since the beginning of this century. The development and deployment of slotted anodes in Alcoa industrial cells have been described by Wang et al. [3]. In their work, the overall gain obtained by the slot implementation in the smelters ranged from 30 mV to 160 mV, depending on the cell technology. In addition, the voltage noise was also reduced when slots are used. The observed voltage gains variation was dependent on anode current density, anode size and shape, as well as slot type and depth. However, no quantitative function of anode slot impact gain regarding each geometrical parameter or current density could be provided in [3].

In this work, the bubble flow model presented in the previous article [1] has been improved with the inclusion of more geometric features and more appropriate boundary conditions. Then, the new model used in this article is employed to explore the impact of geometrical features and the variation of process parameters on the bubble-induced voltage drop: anode length and width, anode bottom slope, ACD, slot thickness, bath height and nominal current density. The slotted anode configuration chosen is the two longitudinal slotted anode, dividing the anode bottom surface in three equal areas. This configuration is commonly seen in the industry and is frequently used in high-amperage modern cells.

The aim of this research is to produce a set of results that can be used to formulate a curve-fitted analytical equation to predict the bubble-induced voltage drop for any anode configuration within a specified validity interval. These intervals are proposed based on realistic ranges observed in the industry. By using this predictive equation, process engineers can quickly estimate the bubble voltage drop component of the cell voltage, with or without slots, for a more accurate and modern description of the cell voltage breakdown contrary to the classical approaches [2, 4], which do not even consider the existence of anode slots; a common industry practice today.

2. Bath Voltage Drop Modelling Due to Bubbles

One of the challenges of bath/bubble flow CFD modelling is the discretization in space and time of the multiphase flow. The mesh must be sufficiently refined near the anode bottom where the bubbles nucleate as shown in Figure 1. Additionally, the growth, coalescence and detachment of bubbles must be accurately captured in the numerical calculation. Similarly, the time step size must be small enough (0.01 s or less) to track all these characteristics of the flow. As a result, each simulation case becomes computationally intensive, requiring 50–100 hours of processing time on a computer with the following configuration: Intel Core i9-14900KF 24-Core Processor 5.6 GHz, 128 GB RAM memory. In Figure 1, views of the mesh size adopted in this work are shown. At the top, the symmetry plane of the bath and anode is highlighted in the zoom. At the bottom of the picture, the same view is shown, but without the anode, to highlight the bath/anode interface refined mesh.

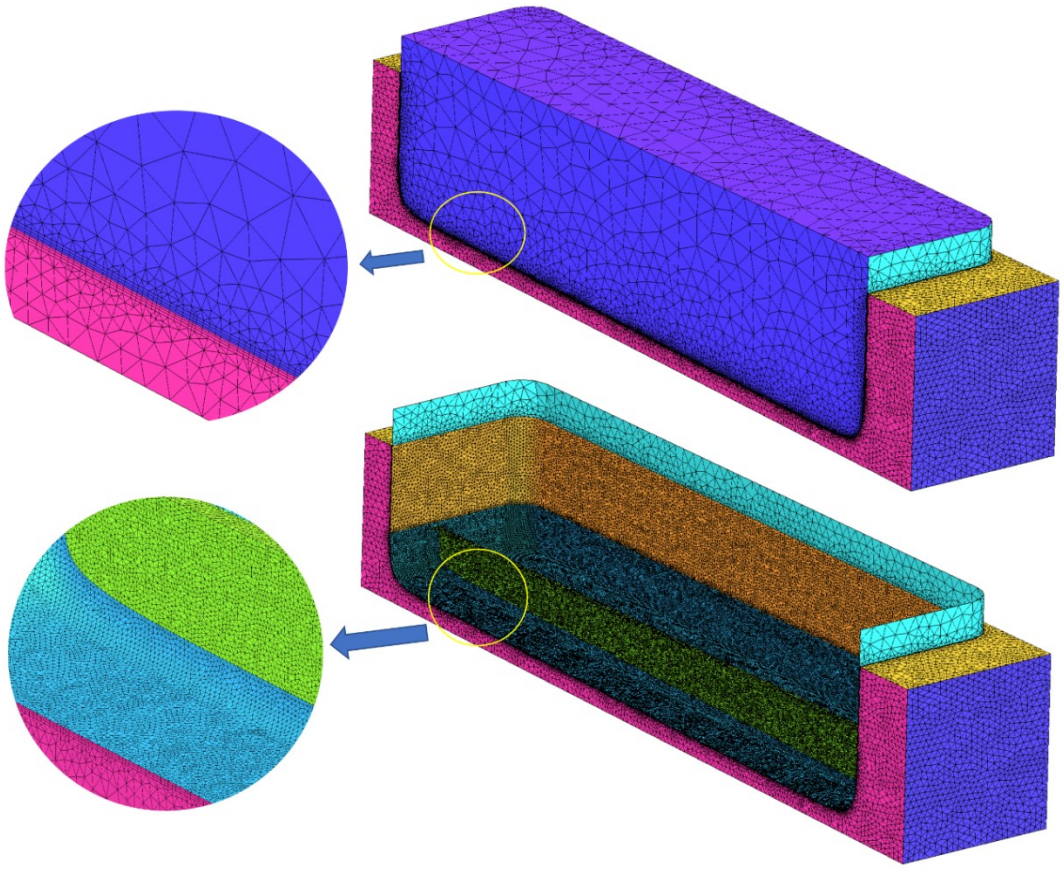

Figure 1. Example of mesh used for transient bubble flow modelling.

2.1 Boundary Conditions and Improvements from the Previous Modelling

In this work, in addition to the bath domain, the carbon anode block is included in the mesh. The half anode domain size is being used as before, allowing for a more realistic boundary condition implementation along with a more accurate current density path. The previous boundary conditions can be found in an earlier work [1]. The improved model boundary conditions are as follows:

- Fluid flow equations:
    - No slip wall boundary condition at anode walls and ledge sidewall for both phases (velocity = 0);

  - Metal/bath interface is set to zero velocity. The presence of interface velocity was studied in the model resulting in no impact on the bubble-induced voltage drop;
  - Bubble generation at anode bottom: The bubble generation is calculated by Faraday's law considering the averaged current density at the anode bottom. The gas generation is uniform in space due to the porous diffusion mechanism in the anode matrix discussed in [5].
  - Gas outlet at the top of the channels space is set by applying an "opening" boundary condition with pressure equal to zero;
  - Symmetries at anode central channel, inter-anode channel and anode center plane.

- Electric potential equation:
  - At the metal bath interface, voltage equal to zero is set, assuming that the metal is equipotential;
  - Anode top nominal current density is applied:
  - At the ledge wall, zero flux of current density is set.
  - Symmetries at anode central channel, inter-anode channel and anode center plane.

A 2D auxiliary numerical model for a realistic prediction of the anode edge curvature was also developed to produce the realistic anode bottom geometry. The anode shape models have been developed in the past, for example, in the work of Zoric et al. [6], where the anode edge shape is predicted by using a 2D numerical algorithm. In our case, the anode bottom shape is obtained by a 2D finite element sub-model that accounts for the material properties and the polarisation voltages. At the anode/bath interface, each node has assigned a polarisation voltage based on the local current density.

3. Anode Parameters Influencing Bubble Voltage Drop

The main anode geometrical features impacting the gas layer film at the anode bottom and its relative bubble-induced voltage drop are studied by varying size and shape, including current density variation. The studied features include:

- Current density, from 0.75 A/cm^2 to 1.05 A/cm^2;
- Anode length, from 1250 mm to 1850 mm;
- Anode width, from 600 mm to 900 mm;
- Bath height (side channel height, excluding ACD), from 110 mm to 185 mm;
- Anode-to-cathode distance (ACD), from 30 mm to 50 mm;
- Slot width (2 equally spaced slots), from 5 mm to 25 mm;
- Anode bottom inclination, from 0° to 1.5°. Inclination towards the centre channel, this is the expected configuration for modern cells.

The gas flow pattern underneath the anode and the current density distribution on the carbon surface for the base case are shown in Figure 2, with and without slots. The proposed "averaged" anode has dimensions of 1550 mm length, 700 mm width, 160 mm bath height, 1.5° anode bottom surface inclination, 40 mm ACD, and it is subjected to a nominal current density of 0.85 A/cm^2. This is considered as a reference shape for an anode, representing an average of typical sizes found in the industry.

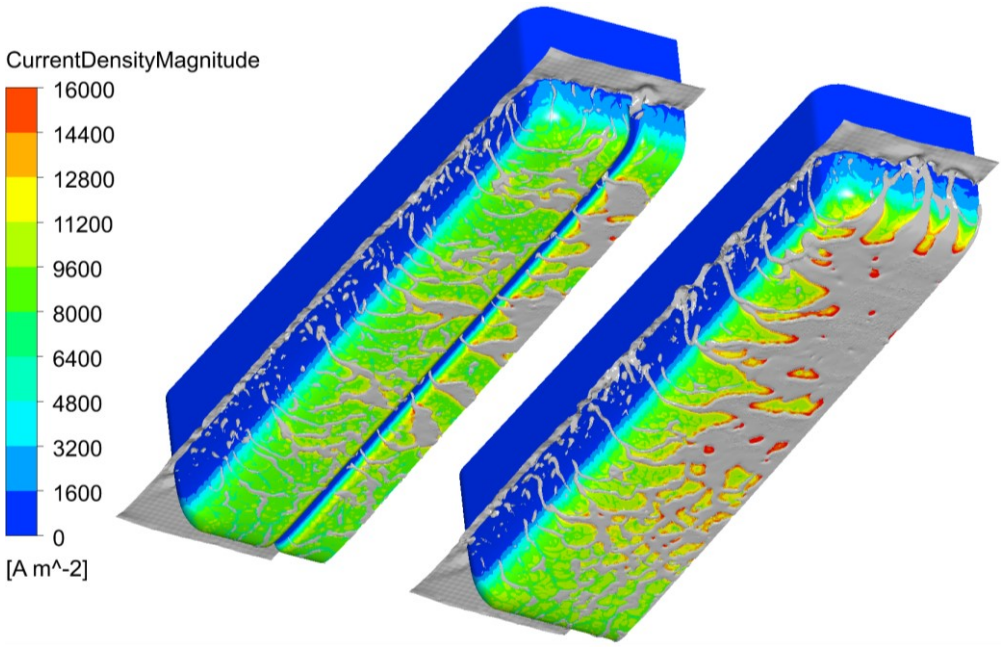

Figure 2. Gas distribution pattern (grey) and anode surface current density (colours). Left: with slots. Right: no slots of the "averaged" anode dimensions. Snapshot after 12 s of simulation time.

It is clear that the bubble coverage is higher in the anode without slots, as the slot drains gas from its vicinity. This makes the bubble-induced voltage drop higher in the no slot "averaged" anode compared with the slotted case: 319 mV against 114 mV. Because the bubble flow is strongly transient and the voltage fluctuates in time (noise), the bubble-induced voltage drop is calculated from the model considering an average over 6 seconds after the flow is developed. This procedure is shown in more detail in the previous work [1]. According to the literature [3, 7 and 8], the bubble noise is observed to decrease with the use of slots. This is also the case in the simulation results of Figure 3, where the standard deviation found in the slotted case is 3.7 mV and for the non-slotted case is 9.3 mV.

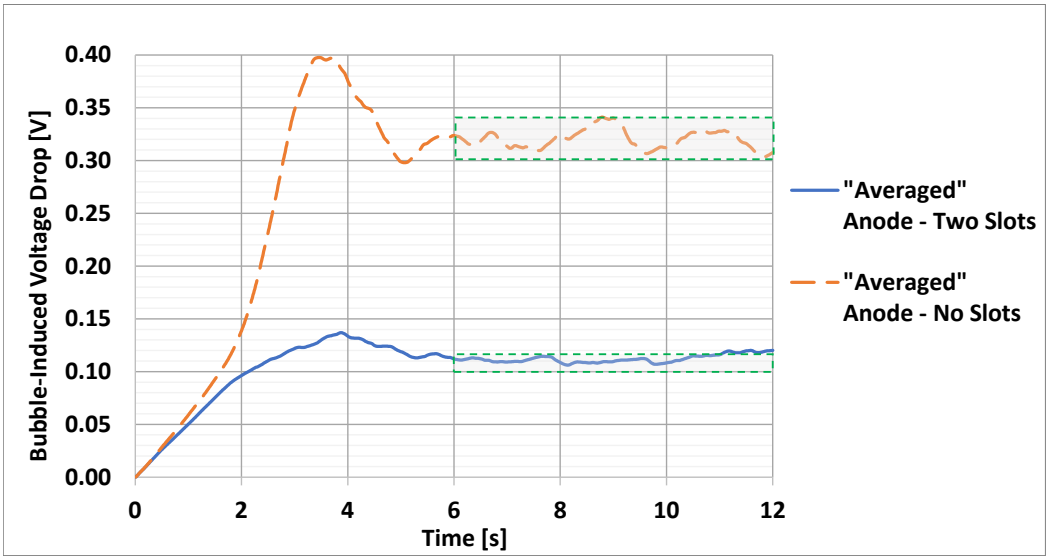

Figure 3. Bubble-induced voltage drop vs time in slotted and non-slotted anodes during the CFD simulation. The green dotted box indicated the period used for voltage drop calculation which was 6–12 s.

The most popular way among process engineers to estimate the bubble-induced voltage is by using the formulae published by Haupin [2], in which findings of many previous studies are compiled. Using these formulae, the bubble-induced voltage reached 295 mV (considering bath composition: CaF_2 5 %, AlF_3 11 %, Al_2O_3 2.5 %, Al_2O_3 Ae 1.8 %). The formulae compilation from [2] is almost insensitive to anode size and was developed for anodes without slots, which were standard when the referenced studies were carried out.

3.1 Current Density

The increase in anode current density is expected to increase the bubble-induced voltage drop due to the combination of two effects:

- As a consequence of Ohm's law, when current increases, the voltage also linearly increases if the resistance is not changed.
- The bubble coverage fraction tends to be higher with a more intense current density because the gas formation rate increases. This actually results in the increase of the bubble resistance, and as a result, the bubble-induced voltage increases faster than the Ohm's law prediction.

Figure 4 presents the gas flow pattern underneath the anode and the current density distribution on the carbon surface for the "averaged" slotted anode subjected to various nominal current density intensities: 0.75 A/cm^2, 0.85 A/cm^2, 0.95 A/cm^2 and 1.05 A/cm^2.

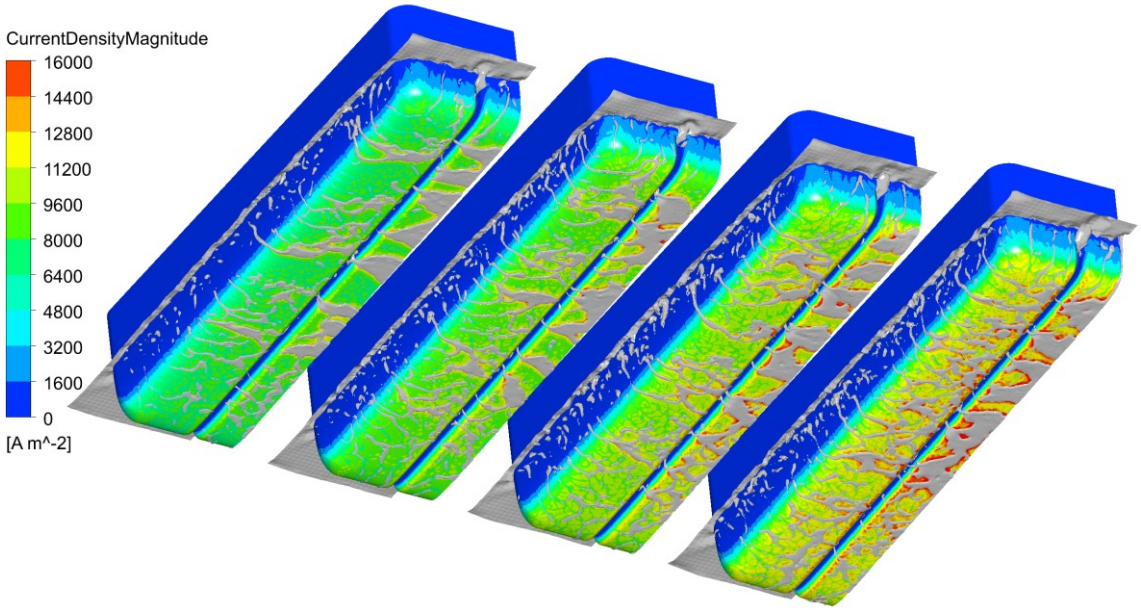

Figure 4. Gas distribution pattern (grey) and anode surface current density (colours) for various current densities. From left to right: 0.75 A/cm^2, 0.85 A/cm^2, 0.95 A/cm^2 and 1.05 A/cm^2. Time = 12 s.

By observing the gas flow pattern, it is possible to visualize a higher gas coverage fraction when the anode is subjected to high current densities. In fact, the calculated bubble coverage fraction for these cases are as follows: 29.3 %, 33.2 %, 31.2 % and 35.1 % for the slotted cases, while for no slot cases, these values are: 42.2 %, 44.5 %, 46.9 % and 48.9 %. Figure 5 presents the resulting bubble-induced voltage drop for different current densities, with and without slots, as well as the values obtained by the literature formulae compilation [2].

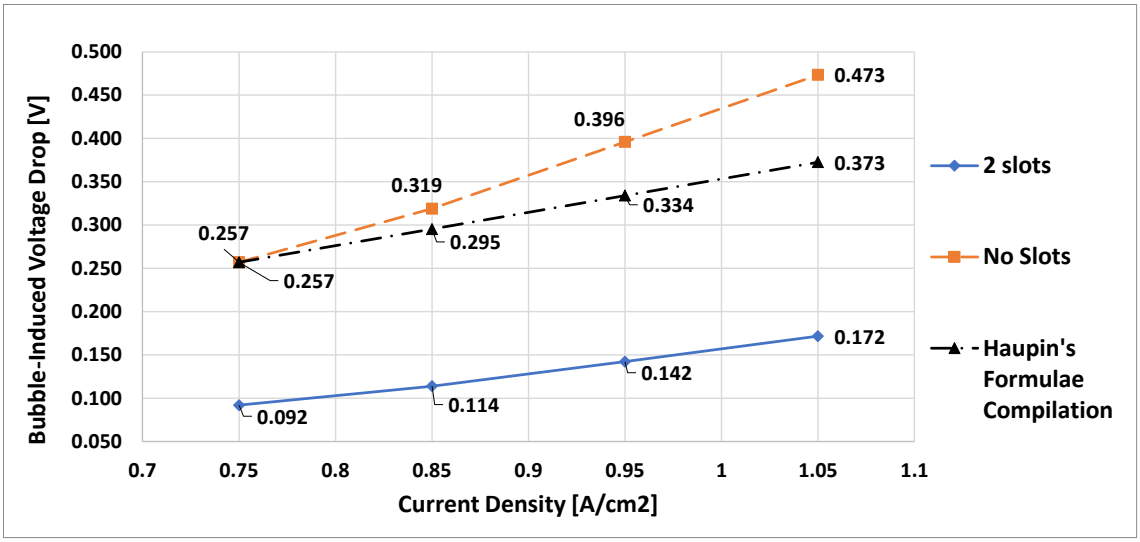

Figure 5. Bubble-induced voltage drop for the "averaged" anode as a function of the current density variation.

The results show a stronger dependence of the voltage drop on the current density calculated by the model when compared with the previous literature, especially in the no slots cases. This is the consequence of the bubble coverage fraction that the simulation is able to capture, in contrast to the classical formulae.

3.2 Anode Length

The length of the anode increases the path and the residence time of bubbles in the bath, potentially affecting the resulting bubble voltage drop. Figure 6 shows the gas flow pattern for the anode with different lengths while maintaining the other parameters as the "averaged" slotted anode.

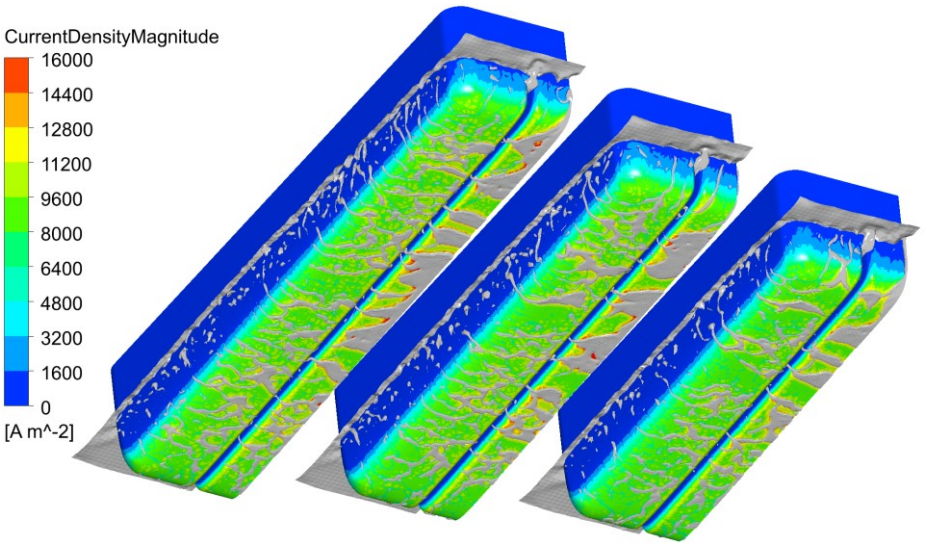

Figure 6. Gas distribution pattern (grey) and anode surface current density (colours) for a range of slotted anode lengths: 1850 mm, 1550 mm and 1250 mm. Time = 12 s.

The shorter anode appears to have slightly less bubble coverage than the longer anode. This difference is reflected in Figure 7, where the bubble voltage drop is plotted for each case with slots, without slots and calculated using the referred literature formulae.

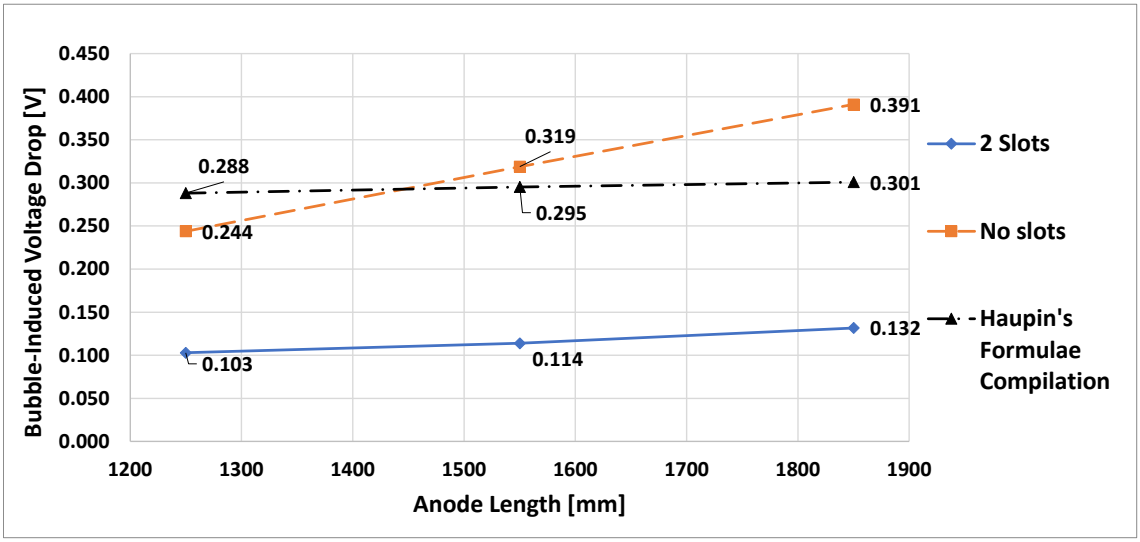

Figure 7. Bubble-induced voltage drop for the anode length variation cases. All other parameters are the same as the "averaged" anode.

As mentioned earlier, the literature formulae are almost insensitive to anode size, in contrast to the values measured in the smelter [3] and the trend observed in simulation results of the current work.

3.3 Anode Width

The anode width is likely to play an important role in the gas dynamics under the anode block. A wider anode subjects the bubbles to a longer path and residence time inside the bath ACD, potentially increasing their induced voltage drop. Figure 8 shows the gas flow pattern for the anodes with different widths while maintaining the rest of the parameters the same as the "averaged" anode.

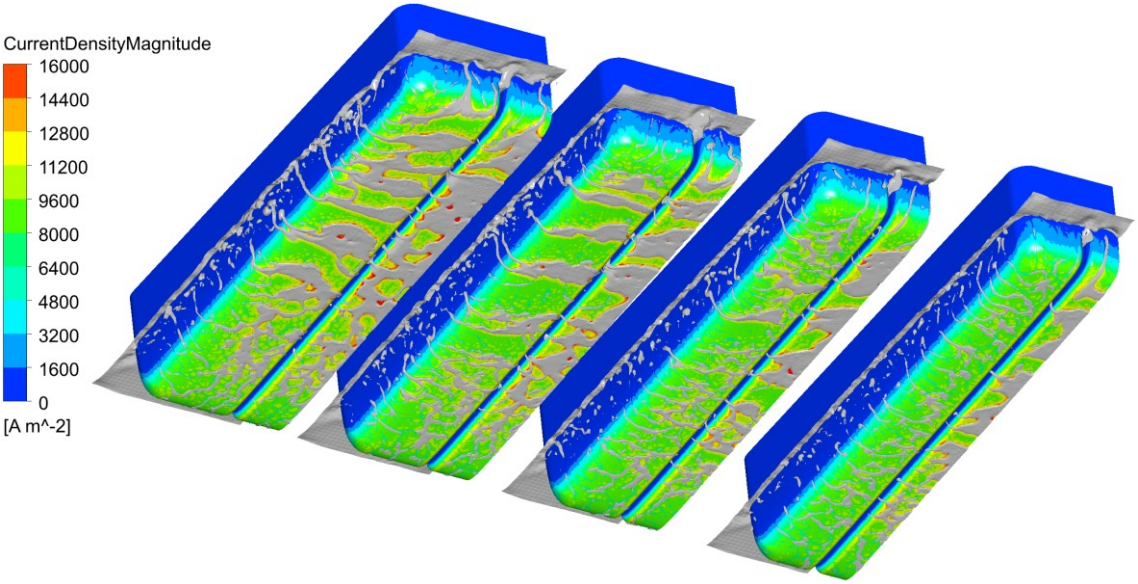

Figure 8. Gas distribution pattern (grey) and anode surface current density (colours) for a range of slotted anode widths: 900 mm, 800 mm, 700 mm and 600 mm. Time = 12 s.

According to Figure 8, the formed bubble sheets are larger under the wider anodes, resulting in an increased gas coverage fraction. Figure 9 presents the bubble-induced voltage for each anode length case, with and without slots along with calculations based on formulae from the referred literature.

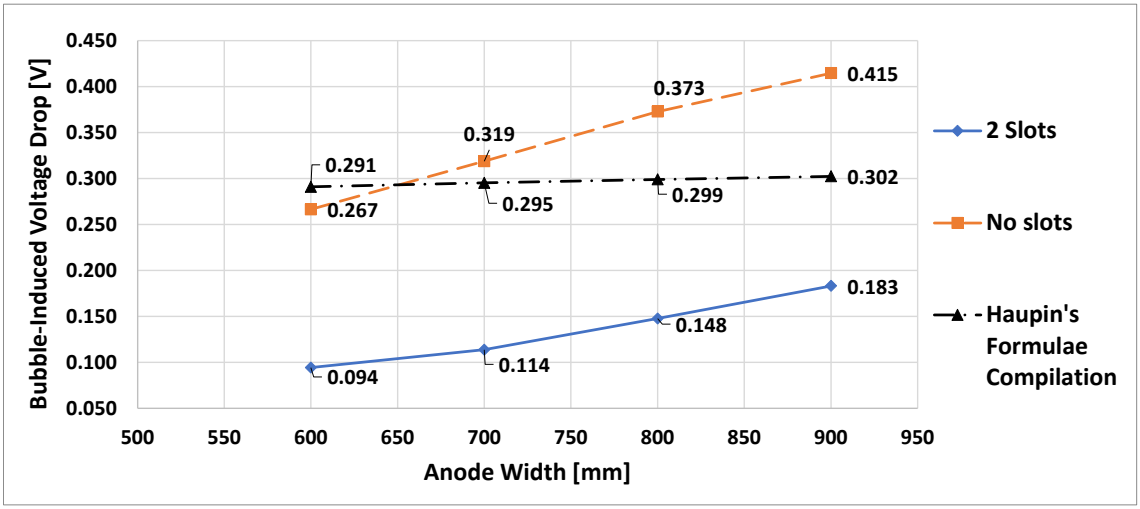

Figure 9. Bubble-induced voltage drop for the anode width variations. All other parameters are the same as the "averaged" anode.

As previously discussed in this work, the predictions show that the bubble-induced voltage drop strongly increases with the anode width, in line with the findings published by Wang et al. [3], and contrary to the results obtained using Haupin's compiled formulae.

3.4 Bath Height

The immersion depth of the anode into the bath creates buoyancy forces responsible for driving the gas towards the exit at the channel's top. The buoyancy force is proportional to the density difference between bath and gas and also proportional to pressure, which in turn increases with the immersion depth. Therefore, the higher the channel, the greater the pressure that the bubbles are subjected to under the anode, potentially accelerating the travel velocity of the bubbles. In this work, the bubbles' voltage drop for a range of bath heights was simulated and the results are shown in Figure 10. The results cover bath heights of 110 mm, 135 mm, 160 mm and 185 mm, while maintaining all other parameters fixed as the "average" anode. Both situations with slots and no slots were calculated including the calculations using the literature compiled formulae. The gas flow picture will not be presented here to avoid repetition as they are all similar to the "averaged" anode case.

The increase of bath height causes a small reduction in the bubble-induced voltage drop due to higher pressure underneath the anode, pushing the bubbles upwards faster. This is observed in both slotted and non-slotted anodes. The literature formulae present almost no impact of the height of bath channels.

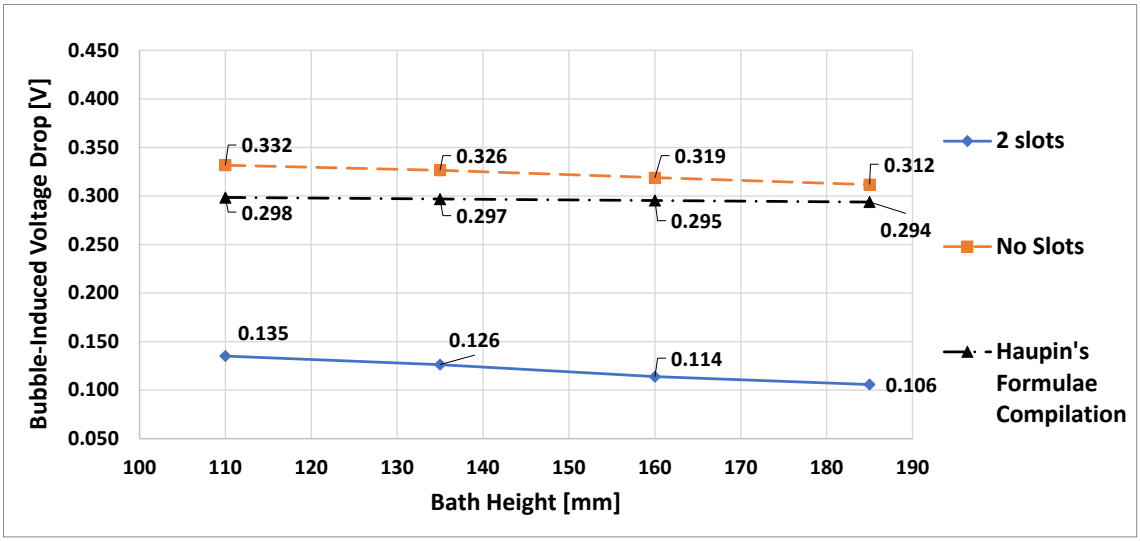

Figure 10. Bubble-induced voltage drop for a range of bath heights. All other parameters are the same as the "averaged" anode.

3.5 Slot Width

The thickness of the slot groove can have two opposite impacts: On one hand a wider slot can facilitate the gas removal and flow from the anode bottom; but on the other hand, the slot thickness reduces the anode bottom area, potentially reducing the benefit of the slot on the bubble voltage drop. In Figure 11, the dotted line presents the isolated effect of the slot thickness variation while maintaining the anode bottom effective area. There is a slight reduction in bubble voltage drop when the slot width is increased from 5 mm up to 25 mm (16 mV total); the voltage seems to stabilize after 20 mm. The solid line in Figure 11 is the resulting bubble voltage drop for cases where increasing the slot width is accompanied with an equal decrease of the anode bottom area, maintaining the anode nominal size, which is a more realistic situation in the industry. Now the optimal bubble voltage drop lies in the range of 10–15 mm slot width.

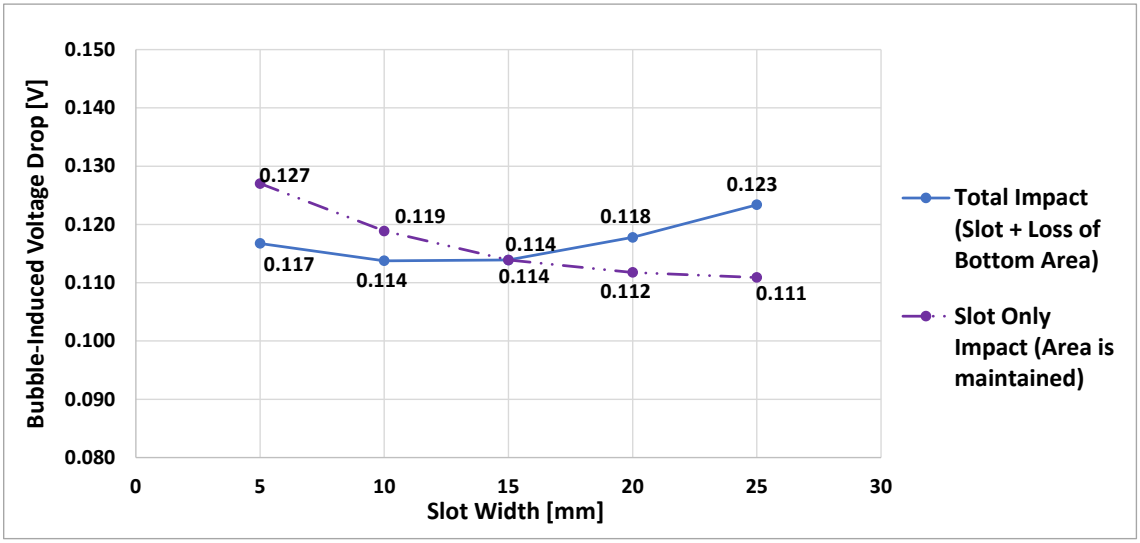

Figure 11. Bubble-induced voltage drop for the slot width variation cases. All other parameters are the same as the "averaged" anode.

Fortunately, most of the aluminium smelters are already using slot widths within or near the optimal range. In any case, the impact of slot width is very small compared to other geometrical factors shown in previous sections.

3.6 ACD (Anode-Cathode Distance)

In this section, the influence of ACD on bubble voltage drop is investigated using the CFD model. The bath bubbles and sheets underneath the anode are believed to be around 5 mm thick [4]. The simulation results confirm this expectation for the bubble sheet thickness (3.5–5 mm) and the shape is comparable to the findings of the experimental work found in the literature [9]. The region affected by the gas is confined to 10 mm close to the anode bottom as presented in Figure 12, where vector velocity and gas bubbles/sheets are presented for the "average" anode at ACDs of 30 mm (top) and 40 mm (bottom). The vectors are plotted on a vertical cut of the bath and anode after 12 seconds of simulated time. The gas bubbles are presented as iso-surfaces inside the entire fluid domain.

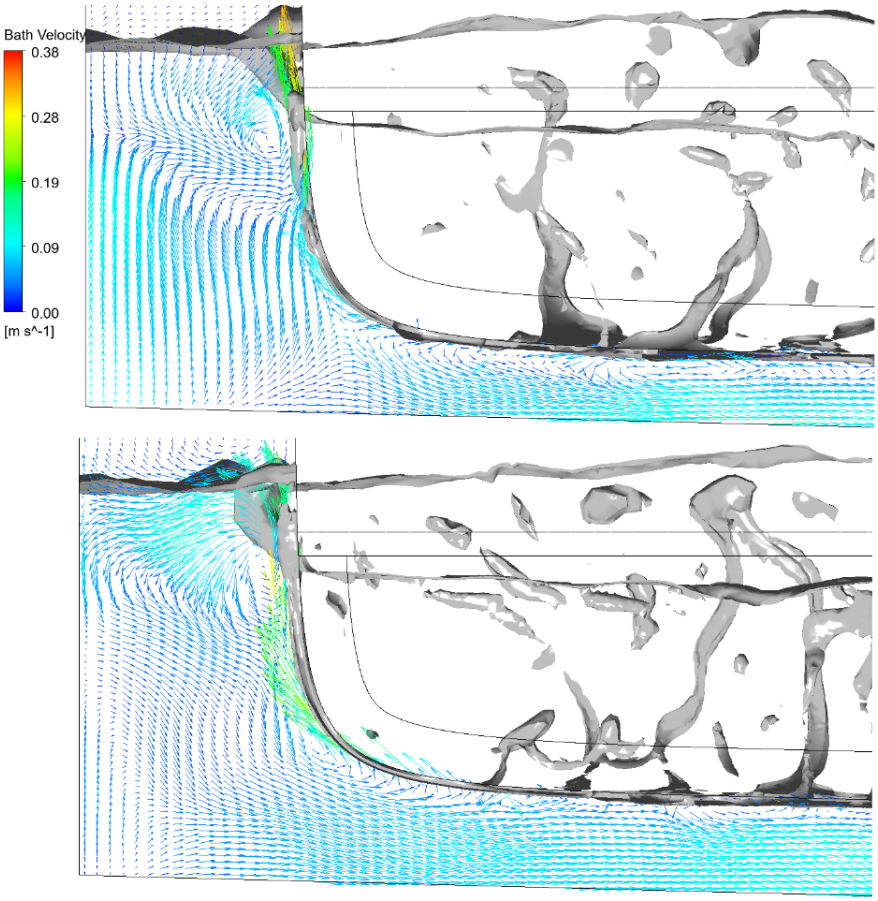

Figure 12. Bath velocity (vectors) and gas bubbles/sheets (grey surfaces) for the averaged anode at different ACDs. Top: 30 mm, Bottom: 40 mm (after 12 s).

In Figure 13, the resulting bubble voltage drop for different ACDs is shown for slotted and non-slotted anodes. The results show a negligible variation in bubble voltage with the ACD, contrary to the full bath voltage drop which indeed is dependent on ACD. Thus, following this reasoning, it can be concluded that the size of the bath channels does not affect the bubble voltage drop either.

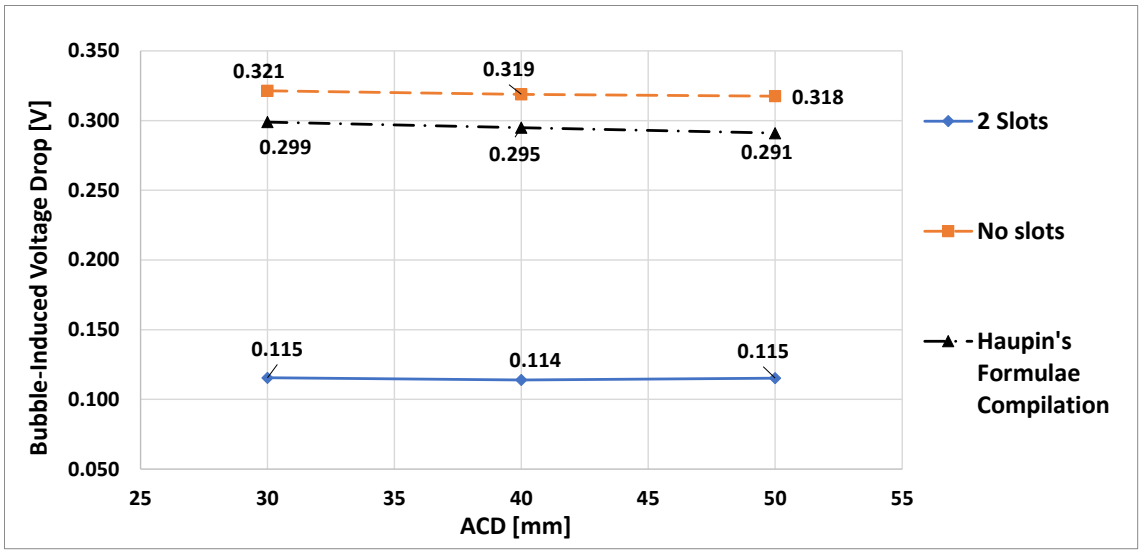

Figure 13. Bubble-induced voltage drop for the ACD variation cases. All other parameters are the same as the "averaged" anode.

3.7 Anode Bottom Surface Inclination

In high-current modern electrolysis cells, the anode bottom surface becomes usually inclined towards the center channel. In fact, the inclination angle follows the metal/bath interface deformation, which is governed by the magnetohydrodynamics (MHD) of the cell [10]. Therefore, in operation, each anode may have a different inclination according to its location. On average, observed anode inclinations are in the range of 0.5°–1.5° and a perfectly horizontal anode bottom is very rare to be observed. Figure 14 presents the calculated bubble voltage drop for the anode bottom inclination variation. Perfectly horizontal anodes present a somewhat higher bubble-induced voltage drop, mainly in the non-slotted cases, but the values stabilize for inclinations above 1.0°, which is more commonly found in industrial cells.

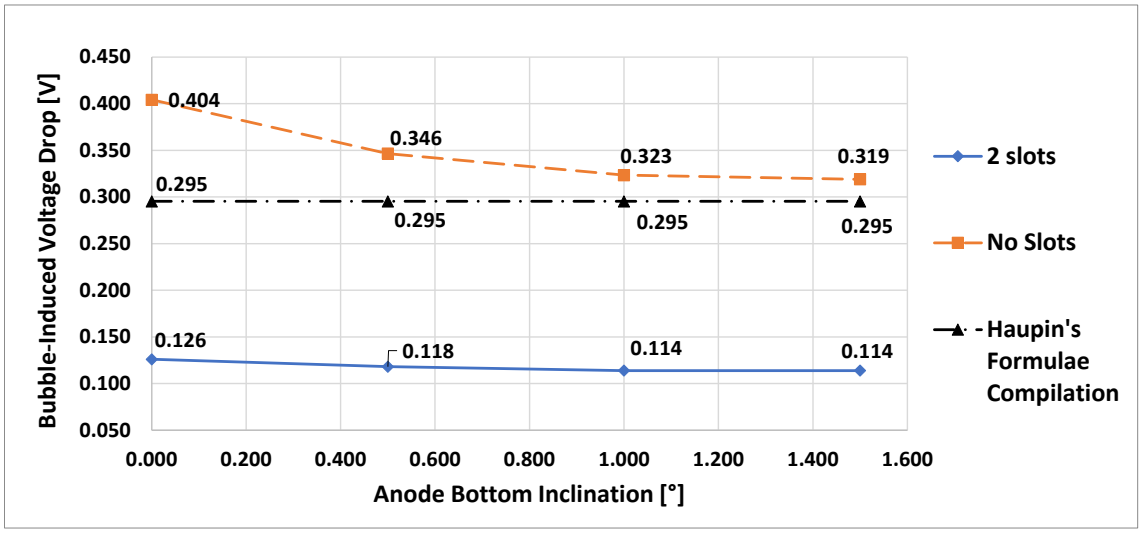

Figure 14. Bubble-induced voltage drop for the anode bottom inclination variation cases. All other parameters are the same as the "averaged" anode.

The Haupin's compilation formulae do not consider anode bottom inclination; and, in Figure 14, the values were simply repeated for comparison. In view of the above results, the anode bottom

inclination influence is small in the modern cells due to the observed metal/bath interface deformation range.

4. Analysis and Correlations

By analysing all the previously discussed results, it has been concluded that the factors that have a significant impact on bubble-induced voltage drop estimations are nominal current density, bath height, anode length, anode width, anode bottom inclination and slot height (compared with the total consumable height). Other studied features, such as ACD and slot width, have minimal or negligible influence within the range of industrial application, and they are not to be considered in a practical equation to maintain as much simplicity as possible. The intervals of validity of this study are as follows:

- Current density, from 0.75 A/cm^2 to 1.05 A/cm^2;
- Bath height, from 110 mm to 185 mm;
- Anode length, from 1250 mm to 1850 mm;
- Anode width, from 600 mm to 900 mm;
- Anode bottom surface inclination, from 0° to 1.5°;
- Slot height (as a weight factor from 0 to 1 of the consumable anode height).
- Two-slotted anodes (or non-slotted anodes) for high-amperage modern cells, with longitudinal slots dividing the anode bottom area into three equal parts.

The voltage drop observed when using partially immersed slots is very similar to the situation with open slots (fully immersed). This was demonstrated in a previous study published by the authors [1]. The equation considers the fraction of time during the anode life (weight multiplier) when the slots are active, and during the remaining time when the slots are consumed the anode acts as a non-slotted anode. The equation was derived through multiple regression of the calculated model results, according to each parameter variation with the help of the *Analyse-it* software tool. A linear multiple regression approach was chosen, except for the anode bottom inclination where the regression is quadratic, because it presented ~ 96–99 % combined correlation, resulting in a simple formula for quick estimations. There was no need to include crossed terms.

For the slotted anodes (2 equally spaced slots), the equation is:

$$V_{b,s} = -0.358 - 0.223\,B_H + 0.277\,C_D + 0.0439\,A_L + 0.298\,A_W + (0.006 - 0.0075\,T + 0.0022\,T^2) \quad (1)$$

where:

$V_{b,s}$ Bubble-induced voltage drop for two-slotted anodes, V
B_H Bath height at the side channel, m
C_D Nominal averaged anode current density, A/cm^2
A_L Anode length, m
A_W Anode width, m
T Anode bottom inclination, °

A similar equation with different coefficients was derived for the non-slotted anodes:

$$V_{b,n} = -0.998 - 0.267\,B_H + 0.766\,C_D + 0.244\,A_L + 0.474\,A_W + (0.083 - 0.1365\,T + 0.0541\,T^2) \quad (2)$$

where:

$V_{b,n}$ Bubble-induced voltage drop for anodes without slots, V.

For the final effectiveness estimation of the slotted anodes inside the cell, the slot duration in the anode life must be considered, which results in a combination of equations (1) and (2).

$$V_{bub} = f_s \cdot V_{b,s} + (1 - f_s) \cdot V_{b,n} \quad (3)$$

where:
V_{bub} Cell averaged bubble-induced voltage drop, V
f_s Fraction of the consumable anode height that has slots, values between 0 and 1.

Combining the equations (1–3), the net voltage gain by switching from non-slotted to two-slotted anodes can be expressed by:

$$V_{Gain} = f_s \cdot \left(-0.563 - 0.044\, B_H + 0.489\, C_D + 0.200\, A_L + 0.176\, A_W + (0.077 - 0.1290\, T + 0.0519\, T^2)\right) \quad (4)$$

where:
V_{Gain} Cell net voltage gain when switching from non-slotted to two-slotted anodes, V.

4.1 Application of the Correlations

In Table 1, a comparison is shown between some extra CFD model results and values obtained from equations (1) and (2) for the same anode cases, varying two parameters simultaneously.

Table 1. Results obtained for crossed variations in slotted and non-slotted anodes. Comparison of the CFD predictions with the results of the proposed equations (1) and (2).

Anode Type	B_H (m)	C_D (A/cm²)	A_L (m)	A_W (m)	T (°)	CFD Model			Volt Equation (mV)	Error	
						Avg. (mV)	SD (mV)	SD (%)		mV	%
Slots	0.11	1.05	1.55	0.7	1.5	188	7.9	4.2	185	-3	-1.8
Slots	0.16	0.85	1.25	0.6	1.5	081	3.2	3.9	075	-5	-6.7
Slots	0.16	0.75	1.55	0.9	1.5	149	3.5	2.4	150	1	0.4
Slots	0.185	0.85	1.85	0.7	1.5	137	5.2	4.2	126	-11	-8.3
Slots	0.11	0.85	1.85	0.7	1.5	134	3.4	2.5	142	9	6.6
No Slots	0.11	1.05	1.55	0.7	1.5	492	9.9	2.0	487	-5	-1.1
No Slots	0.16	0.85	1.25	0.6	1.5	203	7.3	3.6	200	-4	-1.7
No Slots	0.16	0.75	1.55	0.9	1.5	335	6.3	1.9	339	4	1.1
No Slots	0.185	0.85	1.85	0.7	1.5	391	6.7	1.7	387	-4	-1.1
No Slots	0.11	0.85	1.85	0.7	1.5	405	17.7	4.4	407	2	0.5

Despite their simplicity, the equations presented a general accuracy that can be considered reasonably good, and even better for non-slotted anode cases. For the worst case, the error for the predictions from the equations reached 11 mV (8.3 %). This represents a magnitude similar to the calculated bubble noise that reached 17 mV (4.4 %) for the worst case.

5. Conclusions and Future Work

The present modelling represents an improvement over the previous study [1], as it incorporates more consistent boundary conditions and an extended domain where bath and anode are meshed. The model was used to analyse the impact of various anode geometric features and current density on the bubble-induced voltage drop for slotted and non-slotted anodes.

Practical regression fitted equations were derived summarizing all the findings. Process engineers can now use these equations as a tool to quickly predict bubble-induced voltage drop for a range of anodes (slotted and non-slotted) within the validity interval without the need for a complex

numerical model. The present work greatly improves and modernizes the estimation of bubble-induced voltage drop compared with classical literature [2 and 4], as it now considers additional geometric features and slots which were not present in the previously cited works.

Specifically, the modelling results identified the following trends regarding bubble-induced voltage drop:

- There is an important difference in bubble-induced voltage drop between slotted and non-slotted anodes with the same geometric parameters. This was an expected outcome of the CFD modelling already demonstrated before by modelling [1], and by experimental works [3].
- A strong increase in voltage drop of the bubble layer with current density is observed, not only explained by the bath resistance but also because the gas coverage also increases;
- Bubble voltage drop is not sensitive to ACD because the bubble film is too close to the anode surface. The same can be concluded about the width of the bath channels;
- Bubble voltage drop presents a mild decrease with bath height;
- Slot width has a small impact on voltage drop. The optimal slot width range lies between 10 mm and 15 mm, which is already a common industrial practice;
- Bubble voltage drop increases with anode length because the travel distance and the residence time of the bubbles are also increased;
- In the same manner, bubble-induced voltage drop increases with anode width because the travel distance and the residence time of the bubbles are also increased;
- Anode bottom surface inclination slightly reduces bubble voltage drop comparing to horizontal and very low inclination. However, for typical anode bottom inclinations found in modern cells, this parameter is almost neutral.

In this work, results and findings were obtained considering non-slotted versus two-slotted anodes of longitudinal orientation, where the slots are located dividing the anode bottom in three equal areas. By analysing the bubble layer pattern, it is possible to observe higher bubble coverage fraction in the central part of the anode between the slots. A follow-up study could vary the distance between slots to potentially find the optimal distance.

An experimental study is suggested to test the accuracy of the equations provided in this article. Various tests can be conducted on both laboratory and industrial scales to confirm the findings presented here.

6. References

1. Vanderlei Gusberti and Dagoberto S. Severo, Numerical Modelling of Voltage Drop due to Anode Bubbles, *Proceedings of the 41st International ICSOBA Conference,* Dubai, United Arab Emirates, 5–9 November, 2023, *Travaux* 52*,* 1409-1423.
2. Warren Haupin, Interpreting the components of cell voltage*, Light Metals,* 1998, 531-537.
3. Xiangwen Wang et. al., Development and Deployment of Slotted Anode Technology at Alcoa, *Light Metals,* 2007, 299-304.
4. R.J. Aaberg, V. Ranum, K. Williamson and Barry J. Welch, The gas under anodes in aluminium smelting cells Part II: gas volume and bubble layer characteristics, *Light Metals* 1997, 341-346.
5. Sándor Poncsák and László I. Kiss, Role of the porosity of carbon anodes in the nucleation and growth of gas bubbles, *Light Metals* 2018, 1261-1265.
6. J. Zoric, I Rousar, J. Thonstad, Mathematical Modelling of Current Distribution and Anode Shape in Industrial Aluminium Cells with Prebaked Anodes, *Light Metals* 1997, 449-456.
7. Geoff Bearne, Derek Gadd and Simon Lix, The Impact of Slots on Reduction Cell Individual Anode Current Variation, *Light Metals* 2007, 305-310.

8. Ketil Åldstedt Rye, Ellen Myrvold and Ingar Solberg, The Effect of Implementing Slotted Anodes on Some Key Operational Parameters of a PB-Line, *Light Metals,* 2007, 293-298.
9. S. Fortin, M. Gerhardt and Adam J. Gesing, Physical Modelling of Bubble Behaviour and Gas Release from Aluminum Reduction Cell Anodes, *Light Metals 1984*, 721-741.
10. Dagoberto S. Severo, Vanderlei Gusberti, André F. Schneider, Elton C. V. Pinto and Vinko Potocnik, Comparison of various methods for modeling the metal-bath interface, *Light Metals* 2008, 413-418.